Materials Research Bulletin 84 (2016) 462–467

Contents lists available at ScienceDirect

Materials Research Bulletin

journal homepage: www.elsevier.com/locate/matresbu

Short communication

Study of Ga_2S_3 crystals grown from melt and $PbCl_2$ flux

K.A. Kokh[a,b,c,*], Z.-M. Huang[d], J.-G. Huang[d], Y.-Q. Gao[d], B. Uralbekov[e], J. Panomarev[a,c], I.N. Lapin[b], V.A. Svetlichnyi[b,f], G.V. Lanskii[b,f,g], Yu. M. Andreev[b,f,g]

[a] Sobolev Institute of Geology and Mineralogy SB RAS, 630090, Novosibirsk, Russia
[b] Siberian Physical–Technical Institute of Tomsk State University, 634050, Tomsk, Russia
[c] Novosibirsk State University, 630090, Novosibirsk, Russia
[d] Shanghai Institute of Technical Physics CAS, Shanghai, 200083, China
[e] al-Farabi Kazakh National University, al-Farabi Ave., 71, Almaty, 050000, Kazakhstan
[f] Institute of High Current Electronics SB RAS, 2/3 Akademicheskii Ave., Tomsk, Russia
[g] Institute of Monitoring of Climatic and Ecological Systems SB RAS, 10/3 Akademicheskii Ave., Tomsk, Russia

ARTICLE INFO

Article history:
Received 30 May 2016
Received in revised form 22 August 2016
Accepted 27 August 2016
Available online 28 August 2016

Keywords:
A. Chalcogenides
A. Optical materials
B. crystal growth
C. X-ray diffraction
C. Raman spectroscopy
D. Optical properties
B. Phase equilibria

ABSTRACT

Monoclinic and cubic Ga_2S_3 crystals were obtained by Bridgman and flux methods. For the first time optical properties are measured in the bulk samples including THz range. The transparency range 0.44–25 μm is recorded. Ga_2S_3 crystal demonstrated 20 times higher light induced damage threshold compared to GaSe. No phonon absorption peaks are found in the THz range at wavenumbers below 100 cm^{-1}. IR and THz optical, as well as other physical properties render Ga_2S_3 among the prospective materials for THz applications.

1. Introduction

High nonlinear and damage threshold, suitably birefringent crystals are of the top interest in the field of efficient phase-matched mid-IR and THz generation. Among known crystals, pure and doped GaSe possesses a range of attractive physical properties including extreme wide transparency window 0.62–20 μm that continues from 50 μm further into the THz. As a result, GaSe occupied for a long time the upper position among intensively studied crystals for THz application. But its layered structure and resulting poor mechanical properties limit the processing and out-of-door application [1]. Recently, a study of Ga_2S_3 powder has shown its perspectives of application in the IR as a nonlinear optical material [2]. The Ga_2S_3 crystals also have a high photo-sensivity and strong luminescence response. Pure, Fe, transition-metal (Mn) or rear-earth element doped Ga_2S_3 has strong luminescence response all over the visible range [3–6]. It is worthy to note that Ga_2S_3 does not show a luminescence quenching for up to 7 mol% of some light generating impurities. In addition, the ability to convert the UV radiation in solar cells was claimed [7]. Therefore, Ga_2S_3 crystal seems as quite attractive for multidisciplinary applications.

Ga_2S_3 melts congruently at the temperature ~1120 °C. There are three well-known modifications of Ga_2S_3 from early data [8]. The low-temperature modification is white colored, crystallizes in a cubic defect-type sphalerite lattice F-43m. When heated to 550–600 °C, it transforms into yellowish modification, which crystallizes in the hexagonal disordered defect (ZnS or wurtzite-type) lattice $P6_3mc$. At 1020 °C, an orange-yellow modification crystallizes in the monoclinic lattice Cc. The lattice structures of all phases are similar. Their prototype is the ZnS structure with the vacant places of gallium in every third position. Sulfur occupies the positions of almost perfect hexagonal packing and the different ordering in the cation sublattice causes the polymorphism [9].

Nevertheless, there is mismatch in the published data on stability ranges of Ga_2S_3 structures. For example, it was established that the synthesis at 1000 °C from elementary Ga and S and small addition of iodine gave a material with the monoclinic structure at room temperature, while during the heating of this material the structure transition at 987 °C was fixed in situ with the cell parameters a = 3.73053 Å, c = 6.0961 Å [10]. In comparison, these

* Corresponding author at: Sobolev Institute of Geology and Mineralogy SB RAS, 630090, Novosibirsk, Russia.
E-mail address: kokh@igm.nsc.ru (K.A. Kokh).

http://dx.doi.org/10.1016/j.materresbull.2016.08.046
0025-5408/

parameters are close to those of β-phase (hexagonal) [8]. The melt growth of hexagonal phase by the Bridgman method was reported in [11]. In [12] the Ga_2S_3 phase was obtained from reaction between GaI_3 and S at 350 °C and subsequent annealing at 500 °C had led to the cubic phase but further heating to 650 °C resulted in the γ-phase ($P6_1$). The growth of Ga_2S_3 from gas phase in the atmosphere of ICl_3 at 850 °C [7] and the synthesis at 950 °C from Ga_2O_3 and S [2] also had led to preparation of the monoclinic phase. Ga_2S_3 shows anomalous variation in vapor composition with decreasing temperature [13] So, a role of gaseous phase and free-space volume in the ampoule should be concerned. Pardo et al. [14] reported that hexagonal Ga_2S_3 forms in sulfur-deficient conditions in the presence of GaS. Another ambiguity in compiling literature data results from unequal naming of different phases by Greek symbols (α, α', β and γ).

The absence of inversion symmetry in monoclinic structure of Ga_2S_3 suggests application for phase matched frequency conversion. The cubic phase can also be useful for nonlinear applications with the help of a quasi-phase-matching technique [15]. Nevertheless, a very little work on the optical properties and nonlinear application of Ga_2S_3 has been done. It was found that powder of monoclinic and cubic phases exhibit a good transparency in the wavelength range of 0.44–25 μm. The comparatively large SHG effects of, respectively, about 0.5 and 0.7 times that of KTP was also observed, as well as light induced damage threshold is 100 and 30 times to that of AGS. Besides, SHG phase matching at 1910 nm was demonstrated in monoclinic phase powder [2].

The objective of the present work was to evaluate the possibility of obtaining high-quality Ga_2S_3 material and grow bulk Ga_2S_3 crystals by Bridgman and flux methods. Chemical composition, structure, and optical properties over the entire transparency range, for the first time including THz region, were reported.

2. Measurement techniques

The microscopic features and chemical composition of the crystals were determined by a scanning electron microscope MIRA 3 LMU (TESCAN Ltd., Czech) with a dispersion spectrometer INCA Energy 450+ (Oxford Instrument Analytical Ltd., UK) based on a highly sensitive XMax-80 silicon-drift detector at the accelerating voltage of 20 kV and the probe current of 1.5 nA. The most analyses were carried out by using an EM-EDS, the effective time of the spectrum accumulation being 15–20 s. A confocal laser scanning microscope LSM780NLO (Carl Zeiss, Germany) was also used in the study surface morphology of the samples.

Differential thermal analysis was done on the homemade setup based on the S-type thermocouples connected to 2-channel Eurotherm 2604 temperature controller. The charges from synthesized Ga_2S_3 and with addition of $PbCl_2$ were heated/cooled with the rate 600 °C/h several times in order to exclude effects of inhomogeneities. First sample of Ga_2S_3 was analyzed in opened crucible under N_2 flow. The resulting thermogram had several effects with final melting at ~1000 °C meaning a strong evaporation of the sample and the need of closed crucible. Thus other samples were analyzed in sealed quartz ampoules containing ~0.5 g of the charge.

The X-ray diffraction patterns were obtained with a XRD-6000 diffractometer (Shimadzu, Japan) operating with the Cu Kα radiation. Powdered silicon was used as the external standard (a = 5.4309 Å). The diffraction data were collected from 10° to 80° of the 2θ angular range with a step of 0.03° and accumulation time of 1 s per step. The phase composition was identified using PDF4 database.

Vis- and IR absorption spectra of the powdered sample were recorded using the diffuse-reflectance technique. A spectrophotometer Cary 100, Varian (operation range 200–900 nm, spectral resolution of 1 nm) and a FTIR spectrometer Tensor 27, Bruker (375–7000 cm^{-1}, spectral resolution 4 cm^{-1}) were used, respectively.

Laser damage threshold was estimated by visual appearance of defects on the surface of freshly cleaved samples. 10 ns pulses of a Nd:YAG laser were used for irradiation.

THz spectra were recorded by using finished 10 and 20 μm thick Ga_2S_3 wafers glued to 100 μm Si wafers with extra thin layer of epoxy glue and a FTIR spectrometer Vertex 80 v (Bruker, Germany): operation range 5–50,000 cm^{-1}, spectral resolution <0.2 cm^{-1}, wavenumber accuracy <0.01 @ 2000 cm^{-1}, photometric accuracy 0.1% T. The layer of the epoxy glue did not show any absorption structure. Polishing procedure was identical to that described in [16].

The Raman measurements were carried out using a spectrometer InWia (Renishaw, UK) supplied by microscope with magnification 50× at room temperature. Nonpolarized excitation source operating at 532 nm was employed. Both powder and bulk samples were studied. A wide spectral range 100–3000 $см^{-1}$ was analyzed with the resolution 4 cm^{-1}.

3. Material synthesis and crystal growth

All synthesis and growth ampoules were washed up with HNO_3 acid. The starting materials Ga 99.9997 and S 99.99 were additionally purified by remelting under vacuum. To overcome the issue related with high sulfur pressure we used the method proposed for the synthesis of GaSe and GaS compounds [17]. After synthesis the ampoule was broken and polycrystalline white color material was transferred into double wall ampoule.

The unseeded crystal growth was performed by modified vertical Bridgman-Stockbarger methods with heat field rotation [18]. The result of the growth experiment was the crystal 5 cm in length and 8 mm in diameter. A surface of the grown ingot contained many faceted gas cavities. Their reflection of light was simultaneous. Thus, one may suppose that the crystal is a single

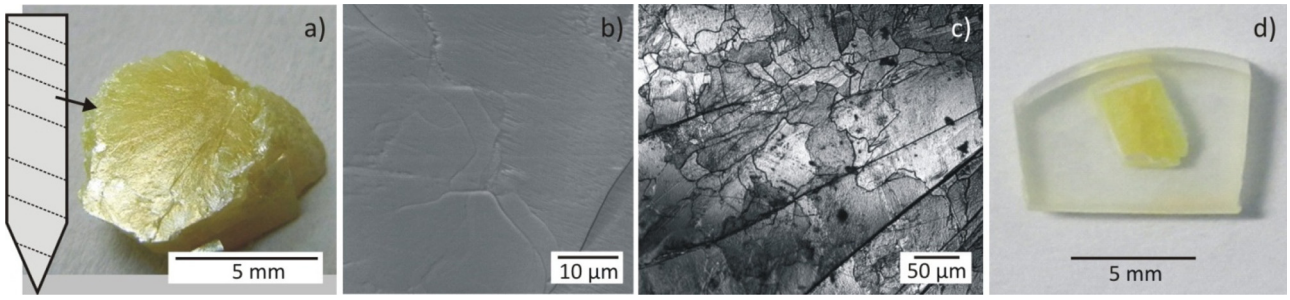

Fig. 1. Melt grown Ga_2S_3: (a) cleaved section from the boule, photos from (b) electron and (c) laser confocal microscopy (scattered light from 405 nm laser), (d) polished plate embedded in polymethylacrelate.

crystalline material. However, the ingot was easily disintegrated due to a large number of parallel cracks suggesting a presence of poor cleavage in the crystal. It seems that milky appearance of the crystals is due to phase transition in Ga_2S_3 during cooling. As a result, the sample consists from small, down to 200 μm, disoriented grains whose boundaries are severe cracked (Fig. 1b, c). Finally, even thin samples look opaque by naked eye (Fig. 1d). EDX analysis showed that composition of Ga_2S_3 has slight excess of Ga relative to stoichiometry: Ga and S contents are 40.49 and 59.51 mol%, respectively.

In order to decrease the temperature of crystallization below phase transition we have used flux crystallization. $PbCl_2$ was chosen as a solvent since it is widely used for the growth of chalcogenides [19,20].

A trial experiment on heating the composition $Ga_2S_3/PbCl_2$ in 1:1 ratio to 1000 °C resulted in full remelting of the sample. XRD analysis showed the presence of initial components only meaning no chemical reaction between the components. After that, a series of samples with various flux concentration were analyzed by DTA. As a result, a phase diagram for the system Ga_2S_3-$PbCl_2$ was constructed (Fig. 2). The liquidus of $PbCl_2$ was assumed according to the known data of the melting point. All samples with addition of $PbCl_2$ have eutectic effect at ~430°C. By extrapolation of liquidus the composition of eutectic may be estimated as ~32 mol% of $PbCl_2$. Further interpretation of DTA data was done using results of XRD analysis of the samples after thermal analysis. Before grinding the samples were soaked in dimethyl sulfoxide to remove $PbCl_2$.

XRD pattern of pure Ga_2S_3 after DTA (Fig. 3d) matches monoclinic modification (Fig. 3b, ICSD card #000160500) and thermal effect at 1000 °C corresponds to polymorphic transition to hexagonal phase. This temperature agrees well with in-situ measurement [10]. The crystal grown from melt by Bridgman method has the same diffraction pattern (Fig. 3c) which confirms the cause of its milky appearance due to phase transition. Same effect at 1000 °C was found for the sample with 10% of $PbCl_2$. Also this and next composition (25% $PbCl_2$) have another thermal effect at ~830 °C. A composition with 40% of $PbCl_2$ does not have this effect since the sample melting is reached at lower temperature ~790 °C.

XRD data gives reliable reason to treat the effect at 830°C as phase transition between monoclinic and cubic modifications. Diffraction profiles of the samples with 10 and 25% of $PbCl_2$ have both monoclinic and cubic peaks (Fig. 3e,f), while the samples with $PbCl_2$ concentration of 40% and more have only cubic pattern (Fig. 3g). It may be assumed that direct transition from monoclinic to cubic structure is not realized in Ga_2S_3. The samples crystallized from pure melt do not contain cubic phase. This may be confirmed by Raman data (Fig. 5). While the appearance of cubic Ga_2S_3 in the samples with solvent may be explained by solute segregation. A melt gradually shifts to $PbCl_2$-rich composition during crystallization. So, after growth of monoclinic Ga_2S_3 the melt falls into the region of primary crystallization of cubic phase. According to DTA the transition in cubic phase takes place at much higher temperature than 550–600 °C referred in previous studies [8]. Besides, the XRD patterns of cubic samples are presented as broadened peaks with maxima shifted from those of etalon ICSD card #76753 (Fig. 3h). All these may be caused by localization of Pb and/or Cl in Ga_2S_3 crystal structure.

In order to perform detailed studies, we have realized the experiment on slow, 1 °C/h, cooling of the charge 50 mol% Ga_2S_3 +50 mol% $PbCl_2$. After removing $PbCl_2$, the sample consisted of yellow octahedra-like crystals (Fig. 4a). They also have cleavage (Fig. 4b), but polished sections are transparent in visible light (Fig. 4c). Chemical analysis revealed a presence of Pb and Cl in the crystal composition, 4 and 2.5 mol%, correspondingly. These impurities explain the shift of XRD peaks for flux-grown cubic Ga_2S_3 (Fig. 3).

4. Optical properties

Raman spectra of the samples obtained both after DTA and crystal growth experiments are shown in Fig. 5. The spectra for bulk and powder samples of monoclinic phase were found to be the same due to disoriented grains in both cases (Fig. 1c). For monoclinic samples. From spectra (a) and (b) it may be concluded that difference in melt cooling rate does not lead to principal changes in the Raman peaks. So, a broadening of major peak at 250 cm^{-1} and appearance of intensive peak at ~290 cm^{-1} may indicate the presence of cubic phase in the sample. However, in one of the previous studies of Ga_2S_3 [21] it was affirmed that Raman spectra of different modifications are indistinguishable due to the likeness of crystal structure.

Increment of $PbCl_2$ concentration in the DTA sample results in the gradual shift of Raman lines. The same effect could be seen for XRD peaks. It may be caused by variation of Pb and Cl

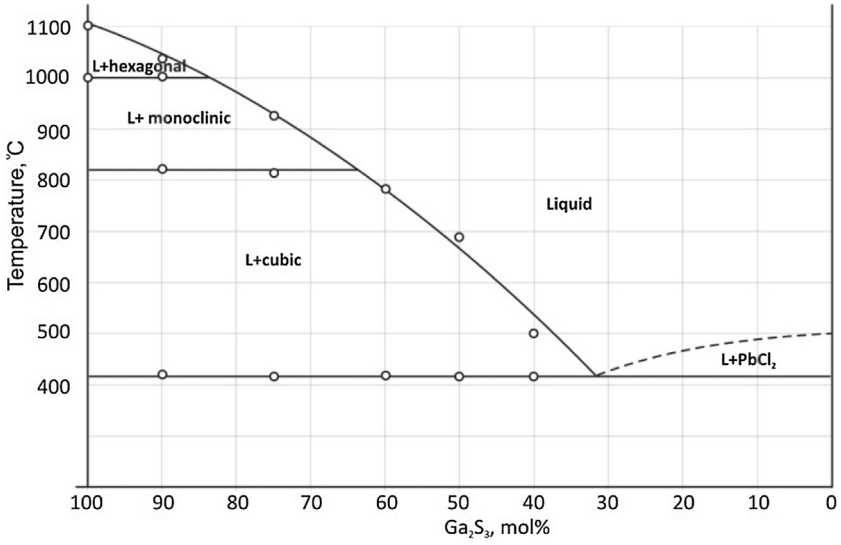

Fig. 2. Ga_2S_3-$PbCl_2$ phase diagram according to the thermal analysis.

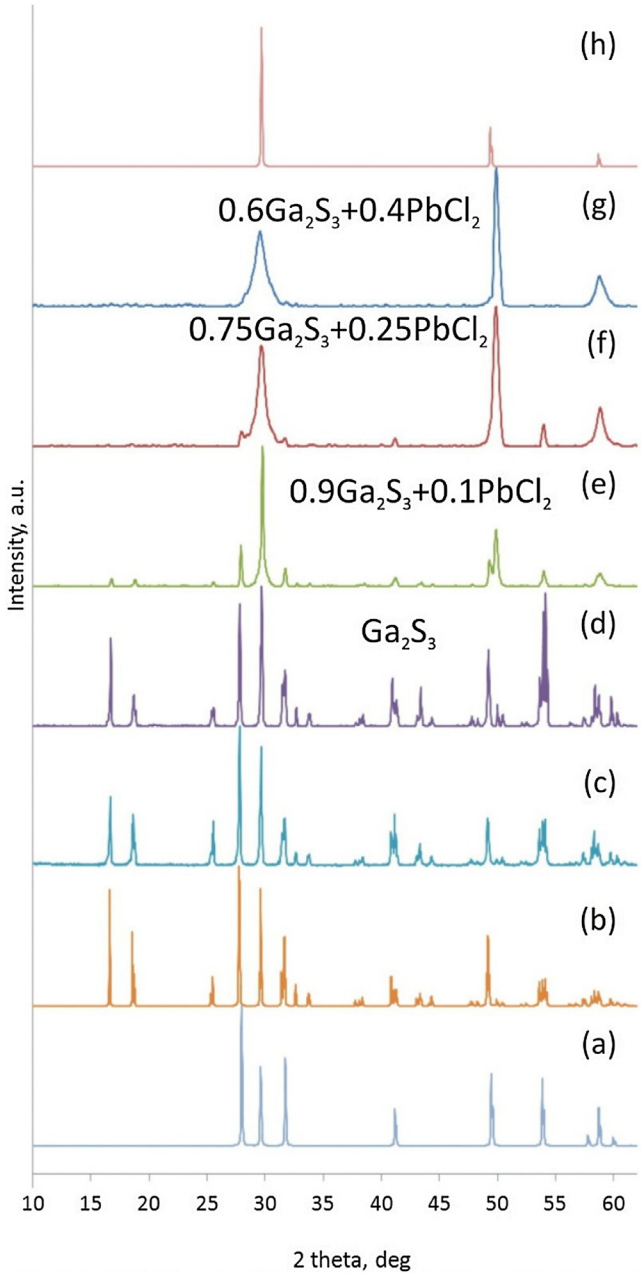

Fig. 3. X-ray diffraction data for Ga_2S_3: etalon patterns for (a) hexagonal and (b) monoclinic phases; (c) after melt growth; (d-g) after thermal analysis of specified composition; (h) etalon pattern for cubic modification.

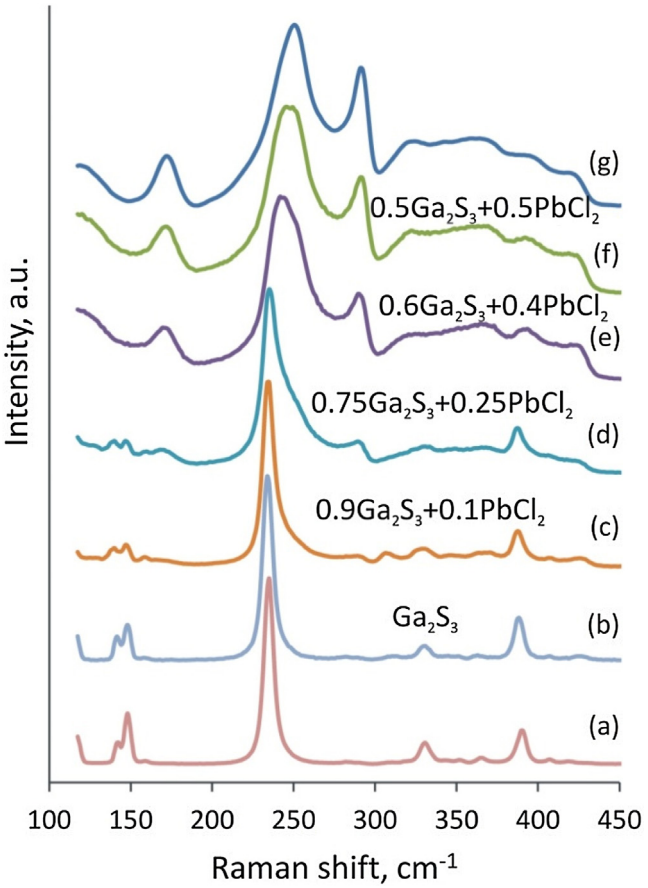

Fig. 5. Raman scattering spectra of Ga_2S_3 after: (a) melt growth; (b-f) thermal analysis of specified composition; (g) slow cooling the composition $0.5Ga_2S_3 + 0.5\ PbCl_2$.

concentration in the Ga_2S_3, which should be gradually decreased with lowering of crystallization temperature. Also, an effective distribution coefficient is quite sensitive to crystallization speed. The latter may be responsible for the difference in Raman lines for composition solidified under 1 and 600°/h (fig. 5f,g).

The main transparency window of monoclinic Ga_2S_3 at "0" level seems to cover 0.44–25 μm range (Fig. 6a). Transmission curves recorded for pure monoclinic Ga_2S_3 powder and diluted with KBr powder, demonstrated the same short-wave 415 nm edge that confirms adequacy of the measurement. This absorption edge was found to be different to that of cubic phase (Fig. 7). For monoclinic phase the value well agrees with recent data of Ho and Chen [7].

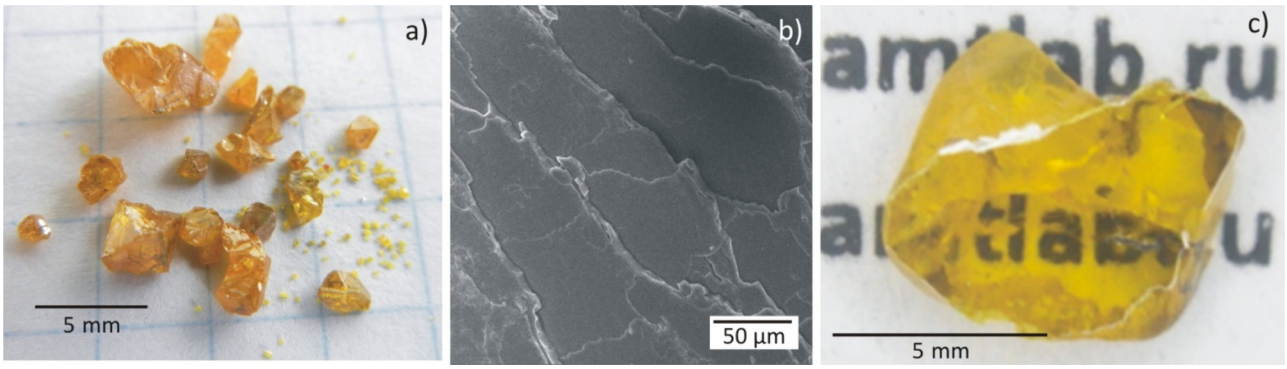

Fig. 4. Ga_2S_3 crystals grown from 50 mol% $PbCl_2$ flux: (a) external view after removing $PbCl_2$; (b) SEM photo of the cleavage; (c) transparent plate for optical measurements.

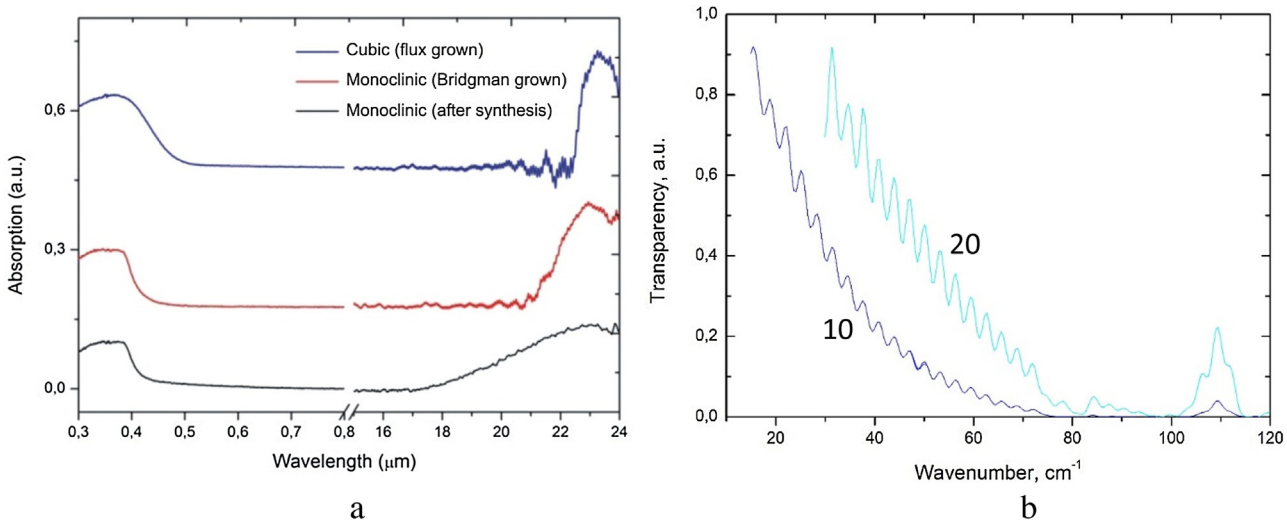

Fig. 6. (a) absorption spectra of Ga_2S_3 samples grown by different methods within main transparency window; (b) transparency spectra of 10 and 20 μm wafers of monoclinic Ga_2S_3 in the THz region.

While the presence of cubic phase may partially explain the existing discrepancy of bandgap values for Ga_2S_3 [22,23].

The maximal transparency window of any studied phase of Ga_2S_3 was found wider than 0.62–20 μm window of GaSe [24]. Besides, the short-wave edge of Ga_2S_3 vanish completely nonlinear (two photon) absorption of Ti:Sapphire and Nd:YAG lasers. No phonon absorption peaks are seen in the THz region below 100 cm^{-1} but etalon patterns (Fig. 6b).

The as-cleaved monoclinic Ga_2S_3 had shown at least 20 times higher damage threshold than a facet of a cleaved GaSe crystal. Both modifications exhibit comparatively large second harmonic (SH) generation effects of about 0.7 and 0.5 times to that of commercial $KTiOPO_4$ (KTP), for the monoclinic and cubic Ga_2S_3 respectively. Calculated birefringence B = 0.0025 [2] is satisfactory high at least for THz generation by down-conversion.

5. Conclusions

Two phases of Ga_2S_3 crystals with different space groups Cc and F–43 m were obtained by vertical Bridgman and flux methods. $PbCl_2$ flux was found to be suitable for growth of transparent cubic phase. However, contamination of flux material induces the search of new solvent for pure Ga_2S_3 growth. The transparency windows 0.44–25 μm of all phases are almost identical and wider than 0.62–20 μm transparency window of GaSe. The short-wave edge of Ga_2S_3 excludes two photon absorption for Ti:Sapphire and Nd:YAG lasers widely used as pump sources for parametric frequency converters. No phonon absorption peaks are available in the THz range at wavenumbers below 100 cm^{-1}. As-cleaved Ga_2S_3 samples demonstrate 20 times higher light induced damage threshold to that for GaSe. Good mechanical properties allow high quality processing and out-of-lab application. Physical properties presented render monoclinic Ga_2S_3 among the most prospective nonlinear materials in IR-THz. However cubic phase may also be applicable in optical rectification devices.

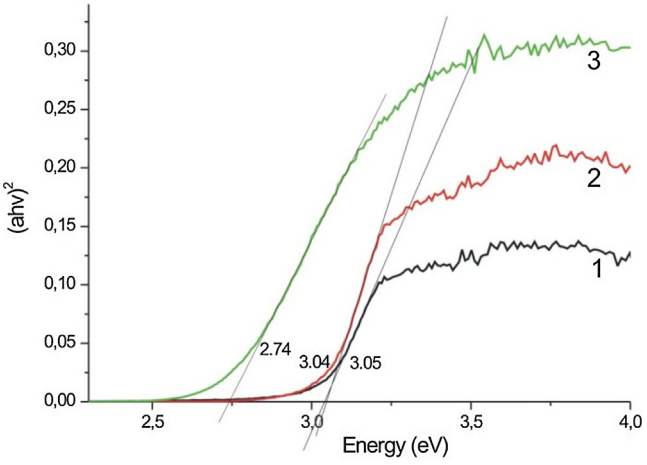

Fig. 7. Optical bandgaps of synthesized (1) and melt grown (2) monoclinic phase, and cubic Ga_2S_3 (3) grown from flux with composition Ga_2S_3:$PbCl_2$ = 1:1.

Acknowledgements

This research was supported by the Russian RSF grant #15-19-10021 (optical measurements) and RFBR grant #16-32-50077 (crystal growth and thermal analysis).

References

[1] J. Guo, J.J. Xie, D.J. Li, G.L. Yang, F. Chen, C.R. Wang, L.M. Zhang, Yu.M. Andreev, K. A. Kokh, G.V. Lanskii, V.A. Svetlichnyi, Doped GaSe crystals for laser frequency conversion, Light Sci. Appl. 4 (2015) e362.
[2] M.J. Zhang, X.M. Jiang, L.J. Zhou, G.C. Guo, Two phases of Ga_2S_3: promising infrared second-order nonlinear optical materials with very high laser induced damage thresholds, J. Mater. Chem. C 1 (2013) 4754.
[3] T. Aono, K. Kase, Green photoemission of α-Ga_2S_3 crystals, Solid State Commun. 81 (1992) 303.
[4] C.S. Yoon, F.D. Medina, L. Martinez, T.Y. Park, M.S. Jin, W.T. Kim, Blue photoluminescence of α-Ga_2S_3 and α-Ga_2S_3: Fe^{2+} single crystals, Appl. Phys. Lett. 83 (2003) 1947.
[5] J.S. Lee, Y.H. Won, H.N. Kim, C.D. Kim, W.T. Kim, Photoluminescence of Ga_2S_3 and Ga_2S_3:Mn single crystals, Solid State Commun. 97 (1996) 1101.
[6] M.S. Jin, Y.G. Kim, H.L. Park, W.T. Kim, Photolumenescence of Ga_2S_3:Ho single crystal, J. Korean Phys. Soc. 39 (2001) S97.
[7] C.H. Ho, H.H. Chen, Optically decomposed near-band-edge structure and excitonic transitions in Ga_2S_3, Sci. Rep. 4 (2014) 6143.
[8] Z.S. Medvedeva, Chalcogenides of Subgroup IIIB of the Periodic System, Nauka, Moscow, 1968, pp. 216 (in Russian).
[9] G. Collin, J. Flahaut, M. Guittard, A.M. Loireau-Lozach, Preparation et structure de Ga_2S_3 α type wurtzite lacunaire, Mat. Res. Bull. 11 (1976) 285–292.
[10] C.Y. Jones, J.G. Edwards, Observation of a phase transformation of Ga_2S_3 in a quartz effusion cell above 1230 K by means of neutron scattering, J. Phys. Chem. B 105 (2001) 2718.

[11] A.T. Nagat, F.S. Baharbi, R.H. Orainy, M. Abou Zied, S.E. Al-Garni, W.S. Al-Ghamadi, Growth and transport properties of some gallium chalcogenides from the group $M_2^{III}X_3^{VI}$ semiconductor compounds, JKAU Sci. 23 (2011) 31.
[12] V. Vel'muzhov, M.V. Sukhanov, A.M. Potapov, A.I. Suchkov, M.F. Churbanov, Preparation of extrapure Ga_2S_3 by reacting GaI_3 with sulfur, Inorg. Mater. 50 (2014) 656–660.
[13] R. Uram, J.G. Edwards, Vaporization chemistry in the gallium-sulfur system, Thermochim. Acta 204 (1992) 221.
[14] M.P. Pardo, A. Tomas, M. Guittard, Polumorphisme de Ga_2S_3 et dieagramme de phase Ga-S, Mater. Res. Bull. 22 (1987) 1677.
[15] H. Ito, T. Hatanaka, S. Haidar, K. Nakamura, K. Kaewase, T. Taniuchi, Periodically poled $LiNbO_3$ OPO for generating mid IR to terahertz waves, Ferroelectrics 253 (2001) 95.
[16] J.F. Molloy, M. Naftaly, Yu Andreev, K. Kokh, G. Lanskii, V. Svetlichnyi, Absorption anisotropy in sulfur doped gallium selenide crystals studied by THz-TDS, Opt. Mater. Express 4 (2014) 2451.
[17] K.A. Kokh, Yu.M. Andreev, V.A. Svetlichnyi, G.V. Lanskii, A.E. Kokh, Growth of GaSe and GaS single crystals, Cryst. Res. Technol. 46 (2011) 327.
[18] K.A. Kokh, B.G. Nenashev, A.E. Kokh, G.Yu. Shvedenkov, Application of a rotating heat field in Bridgman-Stockbarger crystal growth, J. Crystal Growth 275 (2005) E2129.
[19] E. Post, V. Kramer, Crystal growth of $AgGaS_2$ by the Bridgman-Stockbarger and travelling heater methods, J. Crystal Growth 129 (1993) 485.
[20] A.-D. Weber, M. Muller, D. Hofmann, A. Winnacker, Growth stability of zinc selenide bulk crystals from solutions, J. Crystal Growth 184 (1998) 1048.
[21] G. Lucazeau, J. Lorey, Etude vibrationnelle de α-Ga_2S_3, Spectrochim. Acta Part A 1 (1978) 29.
[22] V.P. Mushjnskii, L.I. Palaki, V.V. Chebotaru, Optical absorption in α-Ga2S3 single crystals, Phys. Status Solidi B 83 (1977) K149.
[23] H.A. Shaikh, M. Abdal-Rahman, A.E. Belal, I.M. Ashraf, Photoconductivity studies of gallium sesquisulphide single crystals, J. Phys. D: Appl. Phys. 29 (1996) 466–469.
[24] D.N. Nikogosyan, Nonlinear Optical Crystals: a Complete Survey, Springer, Media, 2005 427 p.